EXPERIMENTAL STUDY OF AN AXISYMMETRIC NONIMPULSIVE TURBULENT JET

N. V. Aleksenko and V. A. Kostomakha

UDC 537.517.14

This article presents additional experimental data on nonimpulsive turbulence. Such turbulence was studied in experiments in [1-5] (two-dimensional flow) and [6-9] (axisymmetric flow). The authors of [1, 2] conducted their investigations with two grids of fine fabric located in one plane and spaced a certain distance apart. The author of [3] used a grid of plates spaced different distances apart in one plane, the flowing having been transverse to the plates. A two-part hydrodynamic grid with rods of different diameters and spacings was used in [4], while a specially-made combination of flat plates and nozzles was used in [5].

Axisymmetric turbulent flow which is nonimpulsive on the average takes place a certain distance from a body in the flow, the resistance of the body being compensated for by a hydraulic motor. In [6], the body was a disk. The resistance of the disk was balanced by the momentum of a jet injected along the symmetry axis of the flow. A ring was used instead of a disk in [7], while the authors of [8, 9] used a streamlined body, the resistance of which was offset by a jet or propeller.

Analyzing these results, it can be stated that the specific method used to introduce the perturbation has a great effect on the subsequent evolution of the turbulent flow – a fact which is of fundamental importance in the mathematical modeling of turbulence. In connection with this, there is substantial interest in experimental results obtained with initial conditions different from those used in [6-9]. In particular, it is interesting to examine experiments in which turbulence was generated by a body more streamlined than those in [6, 7], but less streamlined than those in [8, 9]. One of the "classical" bodies of this class is a sphere, which we will use in our investigation.

Tests were conducted in a low-turbulence wind tunnel with a closed working part 4 m long and characteristic cross-sectional dimensions 0.4 × 0.4 m with triangular inserts at the corners. A sphere of the diameter D = 25 mm was secured on four tungsten wires 0.1 mm in diameter at the beginning of the working part. The sphere was fitted on a tube with an outside diameter of 8 mm and an inside diameter of 6 mm. Figure 1 shows a diagram of the setup, where 1 is the tube through which air was delivered at a controlled rate by way of a regulator from a high-pressure main; 2, bracing wire; 3, sphere; and 4, working part of the wind tunnel. Also shown is the stationary system of cylindrical coordinates that was later used. The origin of the system was located on the rear edge of the sphere.

As functions of the space coordinates we investigated the mean velocity, static pressure, all components of the Reynolds-stress tensor, and the spectral density of fluctuations of the longitudinal velocity component. To do this, we used a complex of thermoanemometric equipment made by the DISA company with one- and two-wire transducers. We also used Pitot tubes and static pressure tubes in the investigation. The measurements were made in the directions indicated by the dashed lines in Fig. 1, where the wires had no effect. The measurements covered the region $5 \leq x/D \leq 100$, while they covered the entire region of disturbed motion with respect to the coordinate r/D.

Statistical analysis of the signals from the hot-wire anemometer was performed with the HISTOMAT-S automatic data analysis system made by Intertechnique. The sensitive element of the anemometer was made of platinized tungsten wire 0.005 mm in diameter and 1.25 mm in length (one-wire transducer) or 1.5 mm in length (two-wire transducer). The flow nozzles were made of medical needles with an outside diameter of 1.1 mm.

The maximum temperature difference between the flow in the wind tunnel and in the jet at x/D = 0 was no greater than 0.7°C. This allowed us to consider the flow to be isothermal, since the initially small difference rapidly decreased even further with subsequent mixing. The distortions of the measurements associated with the limited space–time resolution of the equipment and its inherent noises were of the same order of magnitude.

Novosibirsk. Translated from Zhurnal Prikladnoi Mekhaniki i Tekhnicheskoi Fiziki, No. 1, pp. 65-69, January-February, 1987. Original article submitted December 29, 1985.

 0021-8944/87/2801-0060$12.50

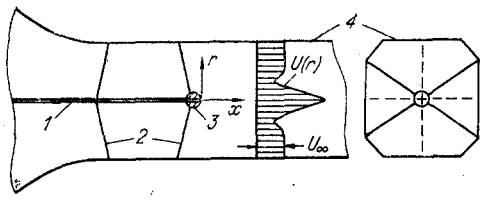

Fig. 1

TABLE 1

ξ	α	U_*^0	σ_1^0	σ_2^0	σ_3^0	e^0	$\frac{\varepsilon^0 D}{U_\infty^3}$	τ^0	η_*
5	—0,022	0,174	0,133	—	—	—	—	—	0,54
7,5	—0,013	0,0837	0,09	—	—	—	—	—	0,64
10	—0,0086	0,0464	0,069	0,055	0,053	0,00534	$7{,}8\cdot10^{-4}$	0,00111	0,735
15	—0,0043	0,0144	0,0469	—	—	—	—	—	0,89
20	—0,0036	0,0022	0,0359	0,0329	0,0329	0,00172	$1{,}07\cdot10^{-4}$	0,000217	1,01
30	—	—	0,0233	—	—	—	—	—	1,255
50	—	—	0,0148	—	—	—	—	—	1,455
70	—	—	0,0105	0,00973	0,00978	0,00015	$2{,}89\cdot10^{-6}$	0,0000047	1,78
100	—	—	0,00768	0,00703	0,00748	0,0000822	—	0,0000026	2,0

The amplitude–frequency characteristic of the entire measurement-analysis complex was nearly uniform in the frequency range 0-20 kHz, which satisfies the test requirements with a margin of safety. However, averaging of the space–time nonuniformities of the velocity field by the sensitive element of the transducer led to a weakening of the fluctuations by 10 and 45%, corresponding to frequencies of 1.9 and 12.5 kHz in the output signal. Most of the energy of the fluctuations (at least 93%) in the spectra of the signals which were studied corresponded to frequencies lower than 1.9 kHz. Thus, with allowance for the rapid decay of the spectrum at high frequencies connected with the factor in question, the error of fluctuation intensity was no greater than 2%. However, when we evaluated the rate of dissipation of turbulence energy, we had to consider frequencies up to 12.5 kHz, and the error due to averaging of nonuniformities by the transducer reached 24%. In connection with this, a correction was introduced for the measurements by the method in [10].

The level of inherent noise in the equipment added to the background turbulence of the wind tunnel, calculated for an equivalent relative dispersion of the velocity fluctuations $\langle u^2\rangle/U_\infty{}^2$, did not exceed $6.5\cdot10^{-6}$. The corresponding corrections were substantial only at the boundaries of the region of disturbed motion, where they were introduced on the assumption that the useful signal and noise were statistically independent.

The random errors for individual experimental points had coefficients of variation no greater than 2% for the averaged velocity, 5% for the intensity of fluctuations of the longitudinal velocity component, 7% for the intensities of the other two components, and 15% for spectral density. The accuracy of the data was increased by a factor of 3-4 when the experimental results were smoothed.

The later-calculated quantity ε – the rate of dissipation of turbulence energy per unit volume – was, as in many experimental studies, evaluated from the isotropic relation $\varepsilon \approx \varepsilon_1 = 15\nu\langle(\partial u/\partial x)^2\rangle$. Meanwhile, the variance of the derivative in this expression was found from measurements of unidimensional spectral density E(k):

$$\left\langle\left(\frac{\partial u}{\partial x}\right)^2\right\rangle = \int_0^\infty k^2 E(k)\,dk.$$

Here, ν is the viscosity of the fluid; u, fluctuation of the longitudinal component of velocity; k, wave number, which on the basis of the Taylor hypothesis was expressed through the frequency of the fluctuations f and the local mean velocity U: $k = 2\pi f/U$.

The error due to the replacement of ε by ε_1, the approximate nature of the relation between k and f, and the limited space–time resolution of the transducer – as well as other factors not considered – can be evaluated from the integral condition of energy conservation in the flow

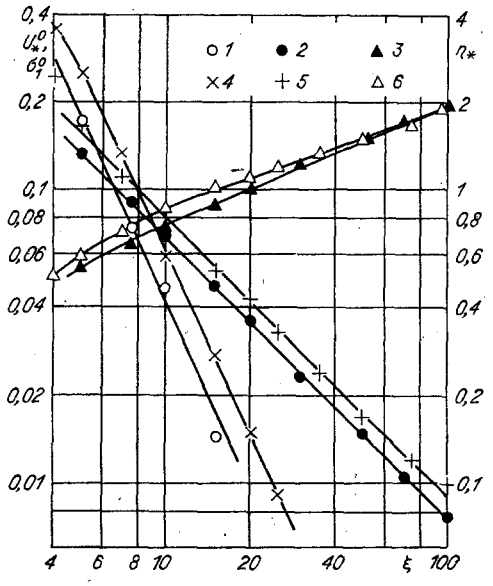

Fig. 2

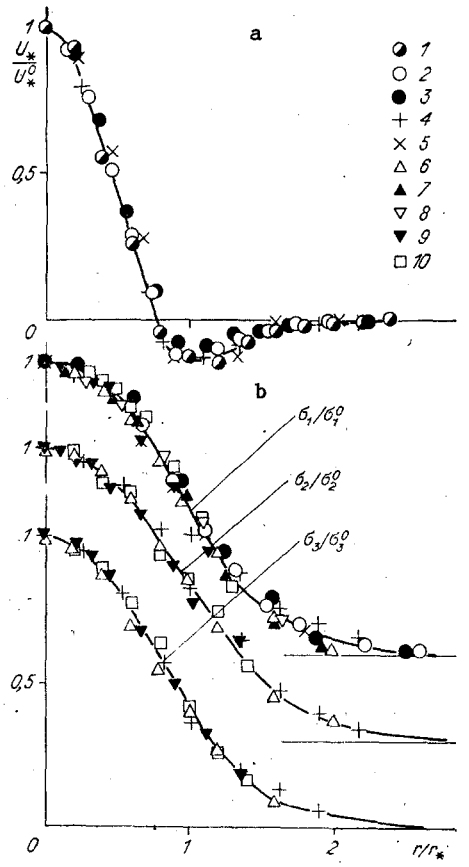

Fig. 3

$$\frac{d}{d\xi}\int_0^\infty (U_*^2/2 + e)\,\eta d\eta = -\frac{D}{U_\infty^3}\int_0^\infty \varepsilon\eta d\eta,$$

where $\xi = x/D$; $\eta = r/D$; U_∞ is the velocity of the incoming flow; $U_* = U/U_\infty - 1$ is the deficit of mean velocity; $e = (\langle u^2\rangle + \langle v^2\rangle + \langle w^2\rangle)/2U_\infty^2$ is the turbulence energy; v and w are the fluctuations of the radial and tangential components of velocity; the brackets denote averaging over time. After introduction of the correction for the limited space–time resolution, this relation was satisfied in the tests with an error no greater than 5%.

The tests were conducted at U_∞ = 15 m/sec. By selecting the rate of air flow into the delivery tube, the drag of the sphere was offset by the momentum of the jet. Thus, with sufficiently large ξ (approximately at $\xi \geq 7$), the following nonimpulse condition was satisfied with an error amounting to no more than 5% of the drag

$$J = \int_0^\infty U_*(U_* + 1)\,\eta d\eta = 0.$$

The drag coefficient $c_x = 8F_x/\rho\pi D^2U_\infty^2$ (F_x is the drag, ρ is the density of the liquid) for a sphere with a delivery tube was determined with zero jet flow from measurements of U_* with sufficiently large ξ, when the following formula is valid with a high degree of accuracy:

$$F_x = -2\pi\rho D^2U_\infty^2\int_0^\infty U_*(U_*+1)\eta d\eta.$$

It turned out to be equal to 0.55, which is somewhat greater than its volume (0.4-0.46, according to different literature sources) for a sphere without a tube and the same Reynolds number ($Re = U_\infty D/\nu = 2.5\cdot10^4$).

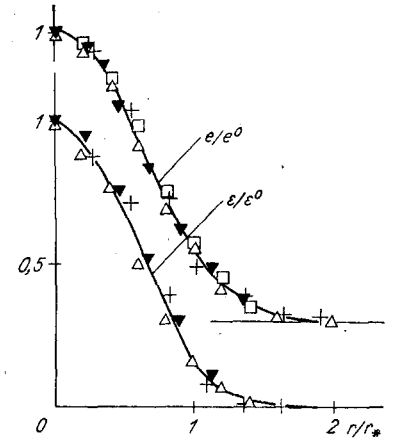

Fig. 4

The experimental data obtained are shown in Table 1 and Figs. 2-4, where the following additional notation is used: $\sigma_1^2 = \langle u^2\rangle/U_\infty^2$, $\sigma_2^2 = \langle v^2\rangle/U_\infty^2$, $\sigma_3^2 = \langle w^2\rangle/U_\infty^2$, $\tau = \langle uv\rangle/U_\infty^2$, the superscript 0 indicating that the quantity pertains to r = 0, $\alpha = 2(p^0 - p_\infty)/\rho U_\infty^2$; p_∞ and p^0 are the static pressures in the incoming flow and in the region of disturbed motion; r_* is the characteristic half-width of the disturbed region, determined by the condition $\sigma_1(r_*) = \sigma_1^0/2$. Experimental points 1 in Fig. 2 correspond to U_*^0; 2, σ_1^0; 3, $\eta_* = r_*/D$; while points 4-6 correspond to the same quantities from [6]. In Figs. 3 and 4, points 1-10 correspond to values of ξ = 2.5, 5, 7.5, 10, 15, 20, 30, 50, 70, and 100.

Conclusions which are in qualitative agreement with the findings in [6-9] can be made on the basis of the experimental data obtained here.

1. In the flow being examined, the disturbances of mean velocity decay more rapidly than the turbulent fluctuations. Thus (see Fig. 2), $U_*^0 \sim x^{-2}$, while $\sigma_1^0 \sim x^{-0.95}$. The proportionality factors in these relations depend on the form and other features of the source of the disturbances. The turbulent shear stresses also decay rapidly (according to the tabular data, $\tau_0 \sim x^{-2.14}$), while the normal turbulent stresses characterized by the quantities σ_1^2, σ_2^2, σ_3^2 differ significantly less from each other than in jets with a nonvanishing excess momentum.

These facts allow us to assume as a first approximation that nearly nonimpulsive turbulent flow which is close to isotropic is established a relatively short distance from the perturbation source.

2. In checking mathematical models of turbulence on this flow, it is necessary to consider that the assertion of isotropy has not been fully substantiated. Comparison of the data in Fig. 3b shows the dependences of σ_1, σ_2, and σ_3 on the coordinate η are somewhat different, and that they do not converge with a further increase in ξ. These differences are not attributable to the measurement error. A similar result was obtained in [11], which was the basis for the study [6].

3. The profiles of the above-examined probability characteristics can be considered self-similar even at short distances from the perturbation source ($\xi > 5$). Usually only two scale functions of ξ – length and velocity – are used in theoretically analyzing similarity properties of free turbulent flows. Examination of a flow with zero excess momentum from this point of view [12] shows that a more general form of the concept of similarity needs to be used for such a flow: with at least one scale function of length and different amplitude functions for different quantities. In Figs. 3a and 4, this function $\eta_* = r_*/D$, U_*^0, e^0, ε^0. The following relations were obtained between these quantities in [12]: $U_*^0/e^0 = \text{const}_1$, $\varepsilon^0\eta_*/(e^0)^{3/2} = \text{const}_2$, $\eta_*/\sqrt{e^0} \sim (x - x_0)$, where $x_0 = \text{const}_3$. The experimental data deviate somewhat from these predictions:

$$U_*^0/e^0 \sim (x - x_0)^{0,1},\ \varepsilon^0\eta_*/(e^0)^{3/2} \sim (x - x_0)^{0,38},\ \eta_*/\sqrt{e^0} \sim (x - x_0)^{1,35}.$$

The value of x_0 in the tests turned out to be close to zero. Not one but two different length scales should evidently be used – as was proposed in [6], to obtain the best agreement in the theoretical analysis.

We express our thanks to the scientific director of the study, V. I. Bukreeva.

LITERATURE CITED

1. A. A. Townsend, Structure of Turbulent Flow with Transverse Shear [Russian translation], IL, Moscow (1959).
2. J. C. Mumford, "The structure of large jet eddies in fully developed turbulent shear flows. Part 1. The plane jet," J. Fluid Mech., 118 (1982).
3. B. Gilbert, "Diffusion mixing in grid turbulence without mean shear," J. Fluid Mech., 100, Pt. 2 (1980).
4. N. V. Aleksenko, V. I. Bukreev, and V. A. Kostomakha, "Nonimpulsive interaction of two isotropic turbulent fields," Zh. Prikl. Mekh. Tekh. Fiz., No. 1 (1985).
5. L. N. Ukhanova and M. O. Frankfurt, "Experimental study of two-dimensional nonimpulsive jets," Inzh. Fiz. Zh., 47, No. 6 (1984).
6. E. Naudascher, "Flow in the wake of self-propelled bodies and related sources of turbulence," J. Fluid Mech., 22, Pt. 4 (1965).
7. A. S. Ginevskii, K. A. Pochkina, and L. N. Ukhanova, "Laws of propagation of a turbulent jet with zero excess momentum," Izv. Akad. Nauk SSSR, Mekh. Zhidk. Gaza, No. 6 (1966).
8. J. A. Schetz and A. K. Jakubowski, "Experimental studies of the turbulent wake behind self-propelled slender bodies," AIAA J., 13, No. 12 (1975).
9. J. A. Schetz, E. B. Daffan, and A. K. Jakubowski, "The turbulent wake behind slender propeller driven bodies at angle of attack," AIAA Paper, No. 133 (1977).
10. J. C. Wyngaard, "Measurement of small-scale turbulence structure with hot wires," J. Sci. Instrum., 1, No. 11 (1968).
11. M. Ridjanovic, "Wake with zero change of momentum flux," Doctoral Dissertation, Philosophy, Iowa, USA (1963).
12. V. A. Gorodtsov, "Similarity and weak closing relations for symmetrical free turbulence," Izv. Akad. Nauk SSSR, Mekh. Zhidk. Gaza, No. 1 (1979).

STUDY OF A DOWNWARD BUBBLY FLOW IN A VERTICAL PIPE

R. S. Gorelik, O. N. Kashinskii, and V. E. Nakoryakov

UDC 532.529.5

The structure of a two-phase gas–liquid flow depends to a significant extent not only on the regime parameters, but also on the geometry of the flow – in particular on the orientation of the channel and the direction of motion of the phases. The flow characteristics are significantly influenced by the distribution of the gas phase across the pipe, as was shown in [1, 2], for example. The form of the profile of local gas content depends on a large number of factors: the dimensions of gaseous inclusions, the magnitude of the gradient of liquid velocity, the intensity of turbulent pulsations of velocity, etc. In many regimes in an upward gas–liquid flow the distribution of local gas content has pronounced maxima near the wall of the pipe; in these regimes, there is a substantial increase in the shear stress on the wall [3]. At the same time, the light particles which surface in the presence of a velocity gradient are subjected to a lateral force directed from the wall toward the center of the flow [4]. In connection with this, the characteristics of upward and downward bubbly flows are quite different.

Here we report results of an experimental study of a downward bubbly concurrent flow in a vertical pipe 15 mm in diameter. The two-phase flow was formed by introducing gas into a liquid with a special mixer which made it possible to obtain a gas–liquid flow with roughly the same size of gas bubbles in each case. Meanwhile, the average size could change in different regimes. Measurements were made with the use of the electrochemical method [2]. The working liquid was a solution of 0.5 N caustic soda and 0.01 N potassium ferri- and ferrocyanide in distilled water. The temperature of the liquid was maintained automatically at

Novosibirsk. Translated from Zhurnal Prikladnoi Mekhaniki i Tekhnicheskoi Fiziki, No. 1, pp. 69-73, January-February, 1987. Original article submitted August 1, 1985.

 0021-8944/87/2801-0064$12.50